



Mapping rice-fallow cropland areas for short-season grain legumes intensification in South Asia using MODIS 250 m time-series data

Murali Krishna Gumma, Prasad S. Thenkabail, Pardharsadhi Teluguntla, Mahesh N. Rao, Irshad A. Mohammed & Anthony M. Whitbread

To cite this article: Murali Krishna Gumma, Prasad S. Thenkabail, Pardharsadhi Teluguntla, Mahesh N. Rao, Irshad A. Mohammed & Anthony M. Whitbread (2016) Mapping rice-fallow cropland areas for short-season grain legumes intensification in South Asia using MODIS 250 m time-series data, International Journal of Digital Earth, 9:10, 981-1003, DOI: [10.1080/17538947.2016.1168489](https://doi.org/10.1080/17538947.2016.1168489)

To link to this article: <http://dx.doi.org/10.1080/17538947.2016.1168489>



© 2016 The Author(s). Published by Informa UK Limited, trading as Taylor & Francis Group.



Published online: 04 May 2016.



[Submit your article to this journal](#)



Article views: 533



[View related articles](#)



[View Crossmark data](#)



Citing articles: 3 [View citing articles](#)



Mapping rice-fallow cropland areas for short-season grain legumes intensification in South Asia using MODIS 250 m time-series data

Murali Krishna Gumma^a , Prasad S. Thenkabail^b, Pardharsadhi Teluguntla^b, Mahesh N. Rao^c, Irshad A. Mohammed^a and Anthony M. Whitbread^a

^aInternational Crops Research Institute for the Semi-Arid Tropics, Patancheru, India; ^bU.S. Geological Survey (USGS), Western Geographic Science Center, Flagstaff, AZ, USA; ^cHumboldt State University, Arcata, CA, USA

ABSTRACT

The goal of this study was to map rainfed and irrigated *rice-fallow* cropland areas across South Asia, using MODIS 250 m time-series data and identify where the farming system may be intensified by the inclusion of a short-season crop during the fallow period. *Rice-fallow* cropland areas are those areas where rice is grown during the *khariif* growing season (June–October), followed by a fallow during the *rabi* season (November–February). These cropland areas are not suitable for growing *rabi*-season rice due to their high water needs, but are suitable for a short -season (≤ 3 months), low water-consuming grain legumes such as chickpea (*Cicer arietinum* L.), black gram, green gram, and lentils. Intensification (double-cropping) in this manner can improve smallholder farmer's incomes and soil health via rich nitrogen-fixation legume crops as well as address food security challenges of ballooning populations without having to expand croplands. Several grain legumes, primarily chickpea, are increasingly grown across Asia as a source of income for smallholder farmers and at the same time providing rich and cheap source of protein that can improve the nutritional quality of diets in the region. The suitability of rainfed and irrigated *rice-fallow* croplands for grain legume cultivation across South Asia were defined by these identifiers: (a) rice crop is grown during the primary (*khariif*) crop growing season or during the north-west monsoon season (June–October); (b) same croplands are left *fallow* during the second (*rabi*) season or during the south-east monsoon season (November–February); and (c) ability to support low water-consuming, short-growing season (≤ 3 months) grain legumes (chickpea, black gram, green gram, and lentils) during *rabi* season. Existing irrigated or rainfed crops such as rice or wheat that were grown during *khariif* were not considered suitable for growing during the *rabi* season, because the moisture/water demand of these crops is too high. The study established cropland classes based on the every 16-day 250 m normalized difference vegetation index (NDVI) time series for one year (June 2010–May 2011) of Moderate Resolution Imaging Spectroradiometer (MODIS) data, using spectral matching techniques (SMTs), and extensive field knowledge. Map accuracy was evaluated based on independent ground survey data as well as compared with available sub-national level statistics. The producers' and users' accuracies of the cropland fallow classes were between 75% and 82%. The overall accuracy and the kappa coefficient estimated for rice classes were 82% and 0.79, respectively. The analysis estimated approximately 22.3 Mha of suitable *rice-fallow* areas in South Asia, with 88.3% in India, 0.5% in Pakistan, 1.1% in Sri Lanka, 8.7% in Bangladesh, 1.4% in Nepal, and 0.02% in Bhutan. Decision-makers can target these areas for sustainable intensification of short-duration grain legumes.

ARTICLE HISTORY

Received 17 December 2015
Accepted 16 March 2016

KEYWORDS

Croplands; cropland *fallow*; seasonal rice mapping; *rice-fallow*; intensification; *khariif*; *rabi*; remote sensing; double-cropping; MODIS 250 m; NDVI; spectral matching techniques; ground survey data; grain legumes; potential cropland areas; South Asia

1. Introduction

A sustainable, profitable, and resilient smallholder agricultural sector is the key to food and nutritional security for the growing populations of Asia and Africa (FAO 2015). South Asia accounts for 40% of the world's harvested rice area (USDA 2010) and feeds almost 25% of the world's population domestically and abroad (FAO 2015). Globally, there is tremendous pressure to produce at least 50% more food to feed the projected world population of 9.15 billion by 2050 (Alexandratos and Bruinsma 2012). There is high demand across South Asia, to increase and diversify food production to meet the increasing nutritional demands of an economically rich and growing population, and to meet export demands that can provide additional income to smallholder farmers. However, increasing production by expanding the area or through technological means such as irrigation, fertilizer, and mechanization is limited due to increasing pressure on croplands for alternative uses as well as environmental concerns, production cost, and severe stresses on water availability in a changing climate scenario (Garnett et al. 2013; Gray et al. 2014). In addition, urbanization, industrialization, and salinization are putting more pressure on existing crop area (Foley et al. 2011). Hence, agronomists consider cropland intensification as an imperative and variable solution.

In India, areas where the *kharif* season (June–October) rainfed rice and/or irrigated rice crops are grown often remain fallow during the *rabi* season (November–February). This is mainly because these lands do not have sufficient water to grow important staple crops (e.g. rice, wheat) during *rabi* season. There is however the opportunity to grow water-efficient short-season grain legumes, which have a high market demand and improve soil health via nitrogen fixation (Dabin et al. 2016; Dixon et al. 2007; Ghosh et al. 2007); this is often termed as rice-fallow intensification.

Spatial information – which can be used to target areas where rice-fallow intensification may be possible – is important for designing effective policies, seed systems, and the provision of extension information (Bantilan et al., forthcoming; Gumma et al. 2014; Kontgis, Schneider, and Ozdogan 2015; Subbarao et al. 2001). Remote sensing is an ideal tool to provide a powerful, quick, and independent approach to estimating *fallow croplands* over large areas and show their dynamics (Badhwar 1984; Lobell et al. 2003; Thenkabail 2010; Thenkabail et al. 2009b; Thiruvengadachari and Sakthivadivel 1997). Over the last 50 years, improved cropland mapping methods and approaches have evolved. There are several studies on spatio-temporal analysis to map agriculture areas by irrigation source (Anderson et al. 2015; Gumma et al. 2011c; Knight et al. 2006; See et al. 2015; Thenkabail, Schull, and Turrall 2005; Velpuri et al. 2009; Xu et al. 2006; Zheng et al. 2015), specific crop type mapping and temporal changes (Foerster et al. 2012; Gumma et al. 2015b; Kontgis, Schneider, and Ozdogan 2015), and crop intensity (Gumma et al. 2014; Sakamoto et al. 2005).

The major aim of this paper is to define a methodology for mapping *rice-fallow* cropland classes for South Asia. *Rice-fallow* areas those where rice crop is grown during *kharif* season (June–October) but are left fallow during *rabi* season (November–February). The uniqueness and novelty of this study are twofold. Firstly, no study has explored mapping fallow croplands using innovative spectral matching techniques (SMTs). This study used every 16-day, MODIS 250 m time-series data (<http://modis.gsfc.nasa.gov/>) for one year (June 2010–May 2011) to map fallow croplands in South Asia using SMTs that were first advocated for cropland mapping by Thenkabail et al. (2007) and later successfully applied in global and regional mapping of croplands (Biradar et al. 2009; Gray et al. 2014; Gumma et al. 2015a; Pittman et al. 2010; Salmon et al. 2015; See et al. 2015; Thenkabail et al. 2007, 2009a, 2012). The study, for the first time, used SMTs to map cropland fallow in order to identify suitable areas for growing short-season (~3 month), low-water-consuming grain legumes such as chickpea, black gram, green gram, and lentils. Second, implementation of SMT methodology to accurately map cropland fallow over large areas, such as South Asia, is invaluable in order to address food security challenges of the twenty-first century.

2. Materials and methods

2.1. Study area

South Asia is located between $5^{\circ}38'40''$ and $36^{\circ}54'30''$ latitudes and, $61^{\circ}05'00''$ and $97^{\circ}14'15''$ longitudes, covering a geographical area of about 477 Mha (Figure 1, Table 1). It has six agro-ecological zones (AEZs): humid tropics, sub-humid tropics, semi-arid tropics, semi-arid, subtropics, and arid (FAO-IIASA 2012). South Asia borders Western Asia, Central Asia, Eastern Asia, Southeastern Asia and the Indian Ocean. It includes six countries: Pakistan, India, Nepal, Bhutan, Bangladesh, and Sri Lanka

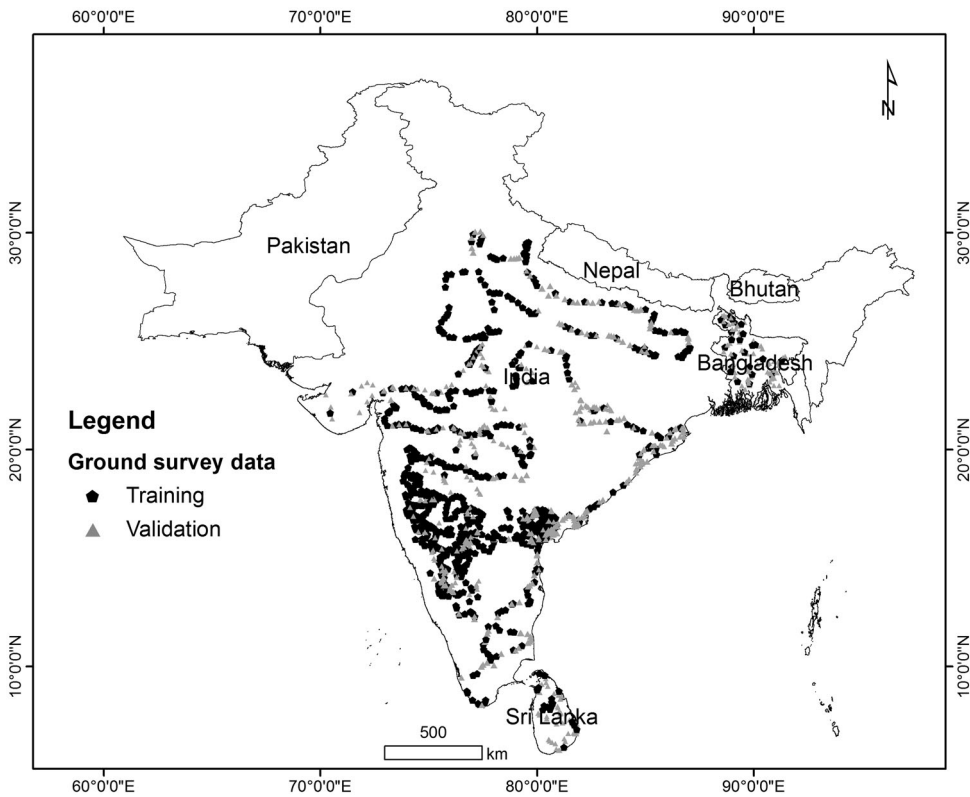


Figure 1. Study area of South Asia and ground data points. There were 1398 cropland data samples of which 303 were used as reference/training data for ideal spectra generation, 527 were used for class identification and labeling, and 568 were for class validation.

Table 1. Cropland areas, rice areas, and geographic areas of the South Asian Nations. Basic country-level geographic areas, cropland areas, irrigated areas, rainfed areas, and rice areas of South Asia for 2010–2011.

Country	Total geographical area ('000 ha)	Total gross planted area ('000 ha)	Net irrigated areas (NAS) ('000 ha)	Net Rainfed areas (NAS) ('000 ha) ^{a,b}	Harvested area of rice ^c (NAS) ('000 ha)
Bangladesh	14,804	15,002	6749	3400	10,801
Bhutan	4365	121	27	94	26
India ^c	345,623	184,443	63,601	104,500	44,712
Nepal	16,210	4208	1926	2100	1560
Pakistan	89,167	22,817	19,270	3600	2377
Sri Lanka	6453	2076	462	1614	832
Total	476,622	228,668	92,035	115,308	60,308

^aSource: World rice statistic, FAO.

^bSource: Rainfed farming system (http://link.springer.com/chapter/10.1007/978-1-4020-9132-2_22) (Hobbs and Osmanzai 2011).

^c<http://www.indiastat.com>.

Lanka. In South Asia, about 80% of the poor live in rural areas and are highly dependent on agriculture for their livelihood (World Bank 2015). There are nine major river basins in the study area: the Indus, Ganges, Brahmaputra, Narmada, Tapti, Godavari, Krishna, Kaveri, and Mahanadi. There are many major and minor irrigation projects connected to these basins in South Asia, covering a total command area of 133 Mha (Thenkabail et al. 2008). However, the ultimate potential of irrigated lands is 139 Mha, the increase being primarily due to the revised assessment of minor ground water schemes and minor surface water schemes to 64 Mha and 17 Mha, respectively. Rice is the major crop in this region, with single or multiple cropping seasons. Most of the rice area (63%) is under irrigated systems, while 37% is rainfed (Gumma et al. 2011a).

2.2. Methods: overview

The methodology is presented in Figure 2 and described below. First, MODIS 250 m NDVI imagery composite of every 16-days was used to create time series for South Asia. Second, ground survey

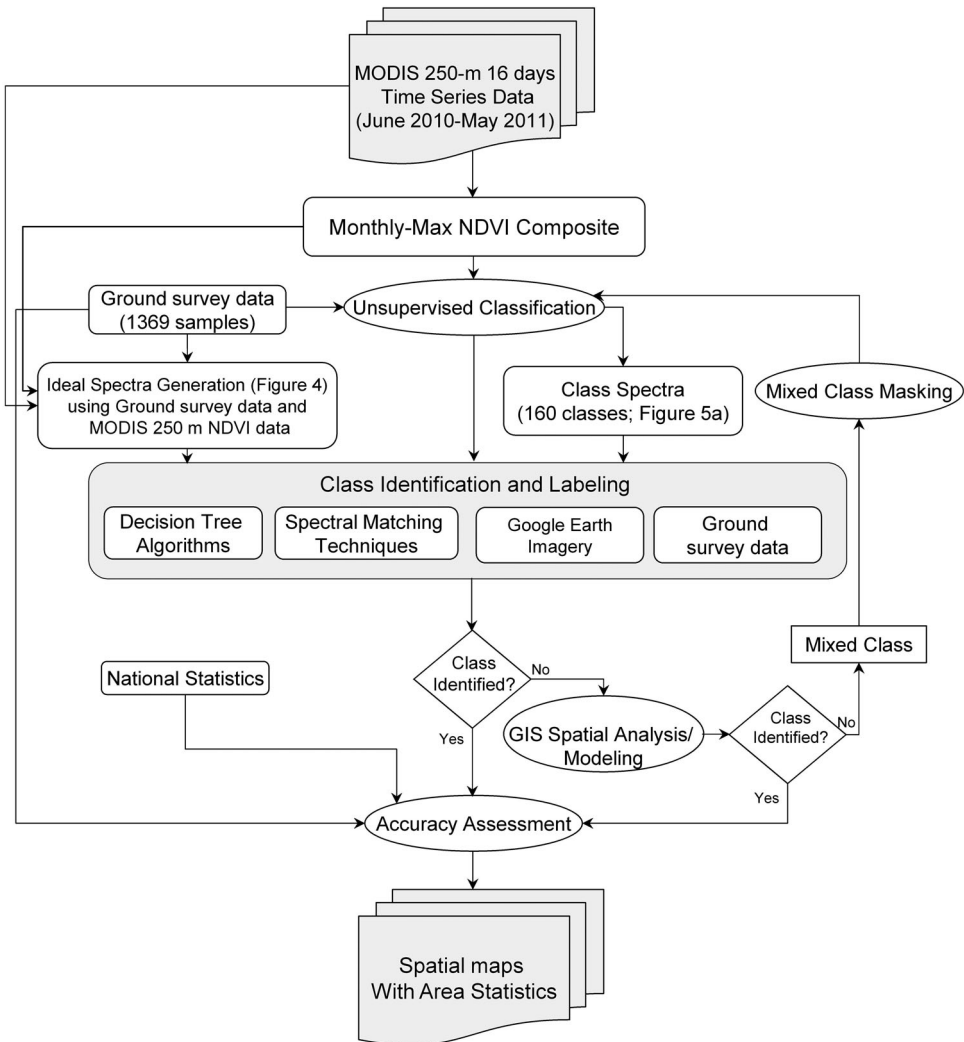


Figure 2. Overview flowchart of methodology. Flow diagram of methodology for mapping *rice-fallow* using the every 16-day MODIS 250 m time-series data, ground data, Google Earth data, spectral matching techniques, and decision trees.

information was collected to gather precise ground knowledge on rice cropping systems of South Asia. Third, ideal spectral generation of rice cropping systems based on precise ground knowledge and by using MODIS 250 m time-series data was performed. Fourth, class spectra were generated using unsupervised classification of South Asia using MODIS 250 m every 16-day NDVI time series. Fifth, the class spectra from the unsupervised classification was spectrally matched with ideal spectra to determine spatial distribution of rice classes across South Asia. Sixth, classes that qualify as rice-fallow areas and short-season grain legumes intensification in South Asia were identified. Finally, accuracy assessments were performed on the products and rice-fallow area estimations were compared with national statistics.

2.3. Satellite data and processing

The present study used MOD13Q1.5 product, which provides every 16-day composite images taken by the MODIS sensor at 250 m spatial resolution. Since rice is the most important crop in South Asia, rice fields are often contiguous and stretch across 100s or 1000s of ha in one stretch (Gumma et al. 2011a; Settle et al. 1996). So, 250 m (6.25 ha) pixels that are acquired every day and processed into 16-day maximum value composites (MVCs) are mostly cloud free, provide excellent wall-to-wall spatial coverage, and have ideal temporal coverage to study crop phenology, vigor, and dynamics (Biggs et al. 2006). The MOD13Q1 product normalized difference vegetation index (NDVI) further normalizes data. Twelve tiles covering the South Asian region were downloaded from the Land Processes Distributed Active Archive Center (LP DAAC) (<https://lpdaac.usgs.gov>). The MODIS re-projection tool (MRT) was used to re-project and mosaic the 12 tiles for each composite date (Gumma et al. 2011a; Thenkabail et al. 2009a). Altogether 23 mosaic images were composited for the crop year 2010–2011 (from June 2010 to May 2011).

The NDVI data were further processed to create monthly maximum value composites (NDVIMVC) for each of the seven months in the *kharif* season, using Equation (1).

$$\text{NDVI MVC}_i = \text{Max}(\text{NDVI}_{i1}, \text{NDVI}_{i2}), \quad (1)$$

where NDVI MVC_{*i*} is monthly MVC of *i*th month (e.g. '*i*' is Jan–Dec). *i*₁, *i*₂ are every 16-day composite in a month.

2.4. Ground survey information

Ground survey information (Table 2) was collected at different times in three distinct field campaigns, which were collectively used to increase the sample size for class identification as well as to assess accuracy (Figure 1). Overall, there were 1398 ground data samples of which 303 were used for ideal spectra generation, 527 for class identification and labeling, and 568 for validation (Table 2). These data were collected based on stratified random sampling. Ground data collection is stratified by road network and randomized by distance traveled (either every 15 minutes of drive or every 10 or 15 or 20 km of drive, depending on road conditions or weather conditions or other field work limitations like safety issues or sensitive locations). Roughly, 20% of all ground data samples were used for ideal spectra generation. Greater time was spent on ideal spectral sample locations for the simple reason of finding a local expert to speak and understand agricultural systems. This was not possible for all 1398 locations, but was successfully done at 303 locations. The rest of the samples were initially equally split (527 samples) for class identification and validation. However, the validation samples increased by another 41 points (reaching a total of 568) since these samples came in almost at the end of class identification; so we just treated them as additional validation samples. Further, of the 1398 samples, 395 were non-croplands samples and the rest 1003 were cropland samples. Of the 303 ideal spectral cropland data samples, there were 204 that were from the ideal spectral category (Figure 4) with the rest 99 being non-croplands. The ground data were extensively

Table 2. Ground data samples used for reference/training and validation. The samples were classified into 11 categories.

Cropland class category	Reference samples for ideal spectra generation	Reference samples for class identification	Validation samples for class accuracies	Total samples
01. Irrigated-SC-rice in <i>kharif</i> -fallow in <i>rabi</i> -fallow in summer	14	16	45	75
02. Irrigated-SC-fallow in <i>kharif</i> -rice in <i>rabi</i> -fallow in summer	9	12	21	42
03. Irrigated-DC-rice in <i>kharif</i> -mixed crops in <i>rabi</i> -fallow in summer	28	42	40	110
04. Irrigated-DC-rice in <i>kharif</i> -rice in <i>rabi</i> -fallow in summer	11	28	58	97
05. Irrigated-TC-rice in <i>kharif</i> -mixed crops in <i>rabi</i> -rice in summer	18	22	74	114
06. Rainfed-SC-rice in <i>kharif</i> -fallow in <i>rabi</i> -fallow in summer	35	23	62	120
07. Rainfed-SC-fallow in <i>kharif</i> -rice in <i>rabi</i> -fallow in summer	12	8	12	32
08. Rainfed-SC-flooded in <i>kharif</i> -flooded in <i>rabi</i> flooded-summer rice	5	5	7	17
09. Irrigated-DC-mixed crops in <i>kharif</i> -mixed crops in <i>rabi</i> -fallow in summer	35	61	102	198
10. Rainfed-SC-mixed crops in <i>kharif</i> -fallow in <i>rabi</i> -fallow in summer	37	39	122	198
Total cropland samples	204	256	543	1003
11. All other Samples (non-croplands, other LCLU)	99	271	25	395
Total ground data samples	303	527	568	1398

Note: SC = single crop, DC = double crop, TC = triple crop, LCLU = land cover/land use.

collected during two growing periods: September 2010 (*kharif* season) and January and February 2011 (*rabi* season). At each sample, information was collected on existing crop type, irrigation type, soil type, and land use land cover (LULC) with a 250 m × 250 m patch size and geolocated with a hand-held GPS unit. Information pertaining to irrigated area surrounding the point was categorized into three classes: small (≤ 10 ha), medium (10–15 ha), and large (≥ 15 ha). Additional information was gathered through interviews with farmers and district agriculture extension officers to determine crop intensities, and type during the previous year. Based on this, ground data were systematically collected by adopting the following approach:

Cropland water methods: irrigated or rainfed

Cropping intensity: single crop (SC), double crop (DC), or continuous crop (CC)

Phenology: *kharif* or season 1 (June–October), *rabi* or season 2 (November–February)

Based on this naming system and convention, each class was named (Table 3). For example, class 6 is: rainfed-SC-rice in *kharif*-fallow in *rabi*-fallow in summer. The 10 cropland classes that will be mapped are listed in Tables 2 and 3 and their MODIS spectral profiles illustrated in Figure 4. Table 2 defines how data were collected during field data. Table 3 defines how these classes are mapped using MODIS data. These classes are further discussed in detail in Section 2.8. Of all the classes that will be mapped, our primary interest will be the *rice-fallow* class (i.e. where rice is grown during *kharif* season or June–October, and left fallow during the *rabi* season or November–February).

Samples covered major cropland areas, which in turn were chosen based on the knowledge of district agricultural extension officers in order to ensure adequate samples of major crops as well as other LULC information, including two photographs from each location. In many sample locations, farmers provided information on planting dates, cropping intensity (single or double crop), and percentage canopy cover for these locations. Additional information was obtained from agriculture and

Table 3. Classes suitable for *rice-fallow*. Rationale for considering classes 1 and 6 for *rabi* season (November–February) as fallow cropland areas suitable for chickpea cultivation across South Asia.

Class description	Considered or not	Rationale
Name	Yes/No	
01. Irrigated-SC-rice in <i>kharif</i>-fallow in <i>rabi</i>-fallow in summer	Yes	These rice dominant croplands during <i>kharif</i> season are overwhelmingly fallow in <i>rabi</i> season, have sufficient moisture/water for growing <i>rabi</i> grain legumes
02. Irrigated-SC-fallow in <i>kharif</i> -rice in <i>rabi</i> -fallow in summer	No	Since this class is already overwhelmingly cropped during <i>rabi</i> season, areas under this class are not available for <i>rabi</i> grain legumes
03. Irrigated-DC-rice in <i>kharif</i> -mixed crops in <i>rabi</i> -fallow in summer	No	Since this class is already overwhelmingly cropped during <i>rabi</i> season, areas under this class are not available for <i>rabi</i> grain legumes
04. Irrigated-DC-rice in <i>kharif</i> -rice in <i>rabi</i> -fallow in summer	No	Since this class is already overwhelmingly cropped during <i>rabi</i> season, areas under this class are not available for <i>rabi</i> grain legumes
05. Irrigated-TC-rice in <i>kharif</i> -mixed crops in <i>rabi</i> -rice in summer	No	Since this class is already overwhelmingly cropped during <i>rabi</i> season, areas under this class are not available for <i>rabi</i> grain legumes
06. Rainfed-SC-rice in <i>kharif</i>-fallow in <i>rabi</i>-fallow in summer	Yes	These rice dominant croplands during <i>kharif</i> season are overwhelmingly fallow in <i>rabi</i> season, have sufficient moisture/water for growing <i>rabi</i> grain legumes
07. Rainfed-SC-fallow in <i>kharif</i> -rice in <i>rabi</i> -fallow in summer	No	Since this class is already overwhelmingly cropped during <i>rabi</i> season, areas under this class are not available for <i>rabi</i> grain legumes
08. Rainfed-SC-flooded in <i>kharif</i> -flooded in <i>rabi</i> flooded-summer rice	No	Since these areas have excess water during <i>rabi</i> , not suitable for <i>rabi</i> grain legumes
09. Irrigated-DC-mixed crops in <i>kharif</i> -mixed crops in <i>rabi</i> -fallow in summer	No	Since this class is already overwhelmingly cropped during <i>rabi</i> season, areas under this class are not available for <i>rabi</i> grain legumes
10. Rainfed-SC-mixed crops in <i>kharif</i> -fallow in <i>rabi</i> -fallow in summer	No	These croplands do not have sufficient moisture/water for <i>rabi</i> grain legumes. Thereby, even though these croplands are fallow during <i>rabi</i> season, are not suitable for <i>rabi</i> grain legumes

irrigation departments for areas not accessible due to road conditions and time constraints. LULC names and class labels were assigned in the field using the protocol (Gumma et al. 2014; Thenkabail et al. 2009b). Determining the areas where rice-fallow occurs is of great importance as illustrated in Figure 3.

2.5. Ideal spectral signatures

Ideal spectral signatures (Figure 4) were generated using every 16-day MODIS NDVI time-series data with precise knowledge on croplands based on extensive ground survey information completed in 2010 and 2011 (Table 2, Figure 1). Ideal spectral signatures were based on 204 unique reference samples available from field data (Table 2). The MODIS NDVI time-series ideal spectral signatures were extracted from each of these 204 ground reference field samples. The 204 reference samples (Table 2) were grouped according to their unique categories and also grouped under major rice systems as shown in Figure 4. The samples were grouped into homogeneous categories that generated ideal spectral signatures taking into consideration cropping intensity, crop type, and cropping systems (Figure 4). Each signature was generated with group of similar samples. For example Figure 4 (a), class 1: ‘01. Irrigated-single crop-rice in *kharif*-fallow in *rabi*-fallow in summer (14)’ signature defines/means: irrigated rice croplands during the *kharif* season followed by fallow during the *rabi* season, and also fallow during the summer season (14 ground samples). The signatures are smoothed to remove noise, if present. Overall, a total of 10 unique cropland classes (Figure 4(a–d)) that are either irrigated (classes 1–5 and 9; Figure 4) or rainfed (classes 6–8 and 10; Figure 4), have differing cropping intensities (e.g. classes 1, 2, 6–8, and 10 are single crop; classes 3, 4, and 9

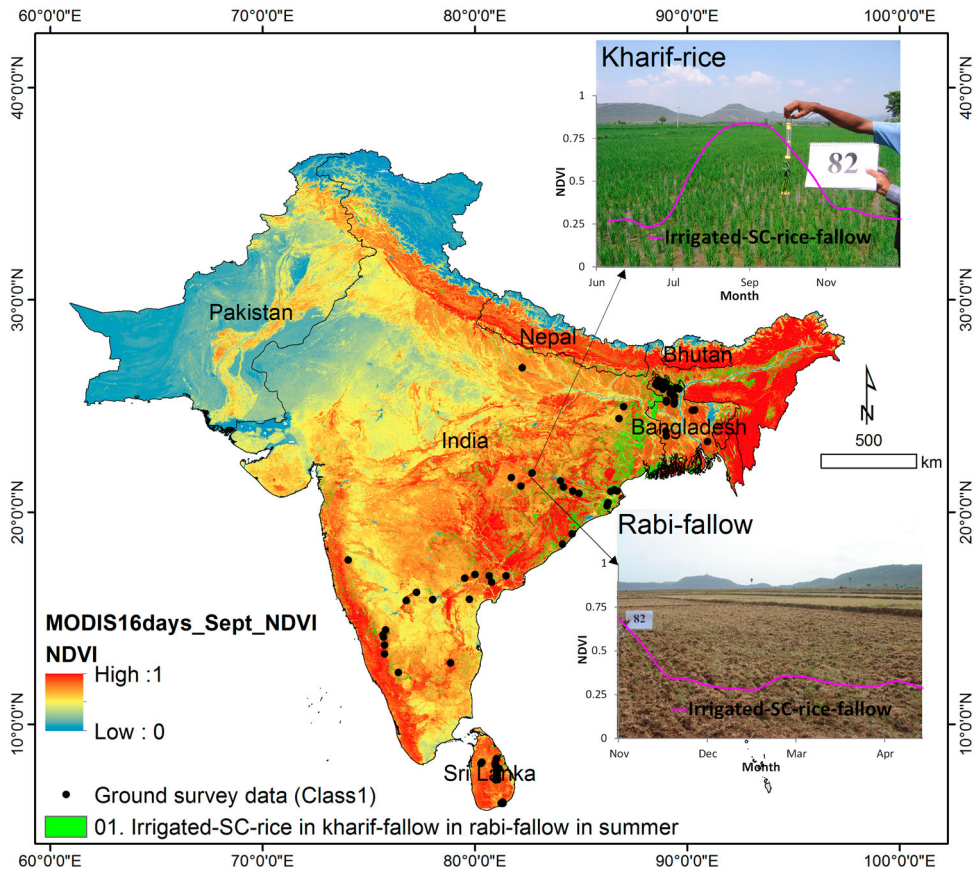


Figure 3. Rice-fallow illustration. *Rice-fallow* are croplands where rice crop is grown during the *kharif* season (upper photo) and left fallow during the *rabi* season (lower photo). Note the MODIS 250 m every 16-day NDVI is also shown on the photo (magenta line) for the different months.

are double crop; and classes 5 is a triple crop; Figure 4), and distinct phenological cycles were established (Figure 4)."

2.6. Class spectra generation

First, South Asian croplands were masked out from non-croplands based on recent findings reported in previous studies (Dheeravath et al. 2010; Gumma et al. 2011a; Thenkabail et al. 2009b). In order to ensure that cropland masks include all cropland areas, we used masks from multiple studies. Given that overwhelming majority of croplands (~99%) are within these cropland masks (that we have verified by overlaying our cropland ground data points), our emphasis of the study was within this mask. Second, even non-cropland mask (all areas outside cropland mask) were analyzed separately to determine whether there were any croplands in the non-cropland mask areas. Third, class spectra (e.g. Figure 5(a)) were generated based on unsupervised classification of MODIS 250 m, 16-day NDVI time-series data for the year 2010–2011 using ISOCCLASS cluster algorithm (ISODATA in ERDAS Imagine 2014™) followed by progressive generalization (Cihlar et al. 1998). Finally, the initial classification was set at a maximum of 160 iterations and a convergence threshold of 0.99, which resulted in 160 classes for entire South Asian study area. For non-cropland mask areas, we performed a quick 25-class classification and looked for any cropland areas. Since any cropland within this was negligible (<1%), we ignored it in our analysis.

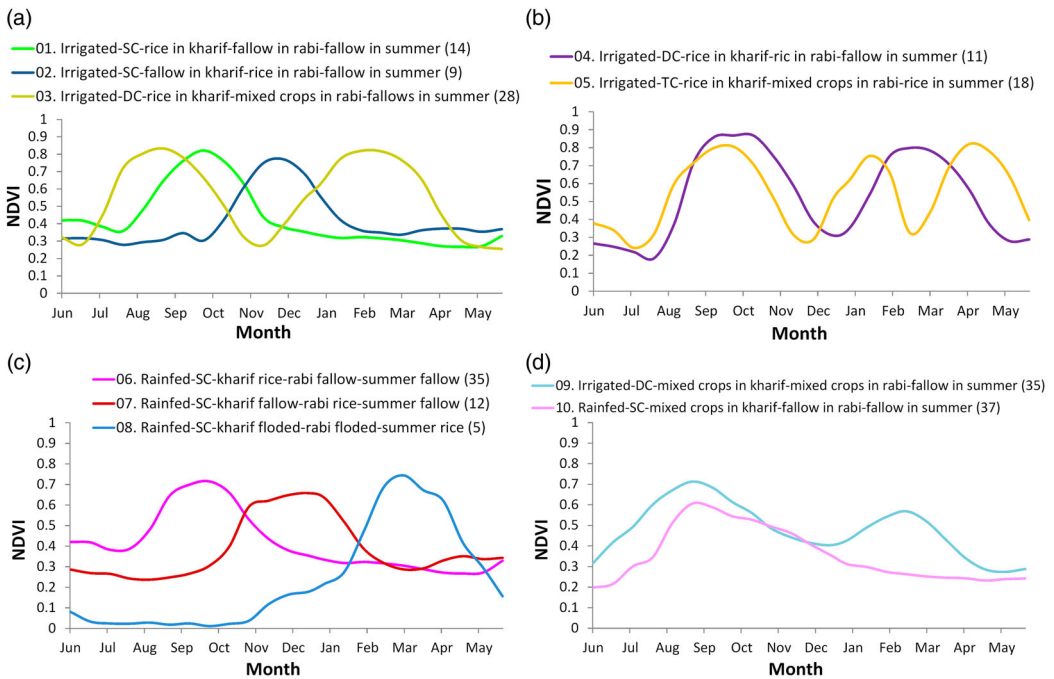


Figure 4. Ideal spectral signatures of 10 cropland classes of South Asia. Here are the 10 ideal spectral signatures. For example, class name in the legend '01. Irrigated, SC, rice in *kharif*, fallow in *rabi*, fallow in summer (14)' (Figure 4(a), green color plot) means irrigated croplands that have cropping intensity of single crop (crop grown only during 1 season in 12 months) with rice crop grown during *kharif* (June–October), but left fallow during *rabi* (November–February) and also left fallow in summer (March–May). The number 14 within bracket means that the ideal spectra is established based on 14 samples that are spread across study area.

2.7. Matching class spectra with ideal spectra to group classes using SMTs

The matching of class spectra with ideal spectra is clearly demonstrated in Figures 5 and 6. The initial 160 unsupervised classes (called class spectra) are grouped into a number of groups based on quantitative SMTs (Homayouni and Roux 2003; Thenkabail et al. 2007). The process involves four steps:

1. Grouping similar class spectra (Figure 5(a)): Starting with initial 160 classes, all classes that are spectrally similar or very close, as determined by qualitative and quantitative spectral matching techniques (QSMTs), are grouped together. In Figure 5(a), we show 12 classes (class numbers: 1, 3, 7, 11, 12, 18, 22, 43, 48, 55, 87, and 121), from the original 160 that were grouped together since they are highly correlated with one another, which is also shown in qualitative plot (Figure 5(a)).

2. Finding an ideal spectra that matches closest to class spectra (Figure 5(b)): From the ideal spectral library (Figure 3), an ideal spectra (Figure 5b) was selected that matches closest to class spectra that are grouped together (Figure 5(a)).

3. Matching class spectra with ideal spectra (Figure 5(c)): The 12-class spectra (Figure 5(a)) were matched with ideal spectra (Figure 5(b)) through QSMT (Figure 5(c)). This led to determining spectral correlation similarity (SCS) *R*-square values (a type of QSMT) by correlating ideal spectra (Figure 5(b)) with class spectra (Figure 5(a)). For example, 'CL_001 (0.83)' means the SCS *R*-square value between class 1 and the ideal spectra is 0.83. The SCS *R*-square values varied between 0.79 to 0.97 (Figure 5c), and

4. Combining all similar class spectral classes into a single class (Figure 5(d)): Since all the 12-class spectral classes are very highly correlated to one another and in turn they are highly correlated with ideal spectra, the 12-class spectral classes are combined into a single class. This single class (magenta in Figure 5(d)) has an SCS *R*-square value of (0.97). So, the 12 classes now become a single

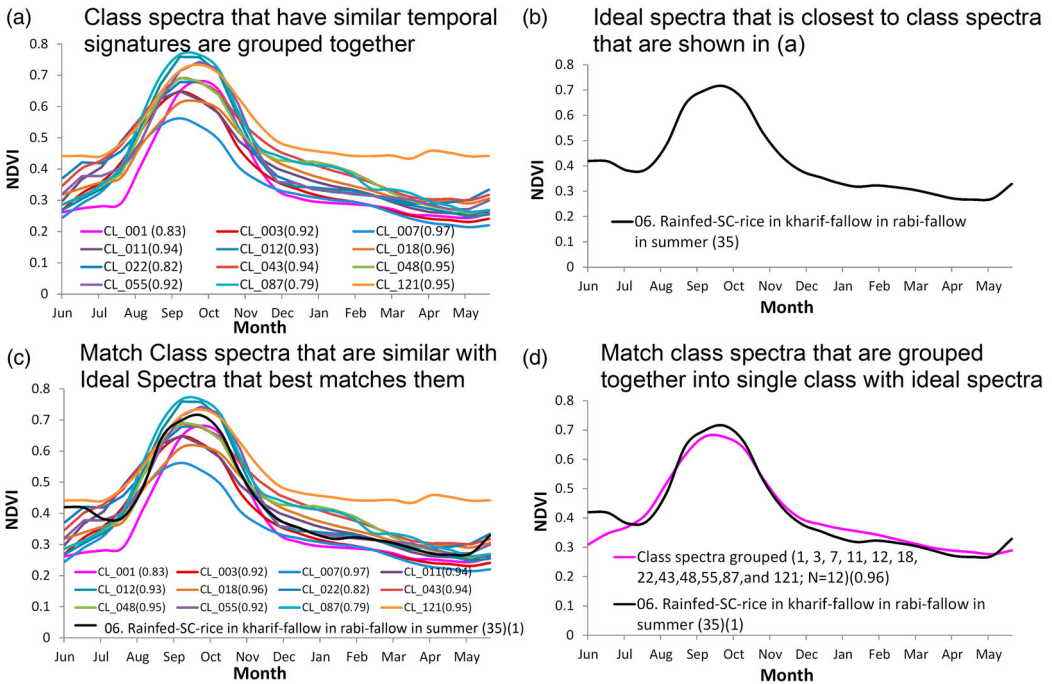


Figure 5. Illustration of spectral matching techniques (SMTs). SMTs to match class spectra with ideal spectra where single crop is grown with rainfed rice crop cultivated during the *kharif* season (June–October), but is overwhelmingly left fallow during the *rabi* season (November–February). The process involves four steps: **(1) Grouping similar class spectra (Figure 5(a)):** For example, of the 160 initial unsupervised classes, we grouped all classes that have similar time-series spectral signatures. For example, in Figure 5(a) a total of 12 classes (class numbers: 1, 3, 7, 11, 12, 18, 22, 43, 48, 55, 87, and 121) were grouped together since they are highly correlated. **(2) Finding an ideal spectra that matches closest to class spectra (Figure 5(b)):** From the ideal spectral library (Figure 3), we selected an ideal spectra (Figure 5(b)) that matches closest to class spectra that are grouped together (Figure 5(a)). **(3) Matching class spectra with ideal spectra (Figure 5(c)):** The 12 class spectra were matched with ideal spectra through quantitative spectral matching technique (QSMT). This lead to determining spectral correlation similarity (SCS) *R*-square value (a type of QSMT) by correlating ideal spectra with class spectra. For example, 'CL_001 (0.83)' means the SCS *R*-square value between class 1 and the ideal spectra is 0.83, and **(4). Combining all similar class spectral classes to a single class (Figure 5(d)):** Since all the 12 class spectral classes are very highly correlated to one another and in turn they are highly correlated with ideal spectra, the 12 class spectral classes are combined into a single class. This single class (magenta in Figure 5(d)) has an SCS *R*-square value of (0.97). So, the 12 classes now become a single class and will have a preliminary name of 'rainfed-SC-rice in *kharif*-fallow in *rabi*-fallow in summer'. This preliminary class labeling was verified with other ground data, and very high resolution imagery to determine the one final label for the 12 combined classes.

class and will have a preliminary name of 'rainfed-SC-rice in *kharif*-fallow in *rabi*-fallow in summer'. This preliminary class labeling was verified with other ground data, and very high resolution imagery to determine the one final label for the 12 combined classes.

Thus, the 12 combined classes take the same label as the ideal spectral, that is, 'rainfed-SC-rice in *kharif*-fallow in *rabi*-fallow in summer'. The spatial distribution of these classes is shown in Figure 6. Also, all non-rice classes (i.e. all other crops) were grouped into a single class as they were not classes of interest in this study. So, the entire focus of this study was in characterizing (e.g. Figure 4), identifying (e.g. Figure 5), and spatially mapping (e.g. Figure 6) rice classes. These preliminary labeling of classes were further validated using: (a) ground survey data, (b) very high-resolution imagery, (c) expert opinion, (d) other published work, or national statistics a combination of these. The same process is used to identify and label all 160 classes, leading to final classes (Figures 8 and 10, and Table 4).

Some classes may not resolve conclusively even after using ground survey information and other information mentioned above. Such classes were then subset, re-classified, and re-analyzed following the protocols mentioned above (Gumma et al. 2011a, 2014; Thenkabail et al. 2007). Using the same

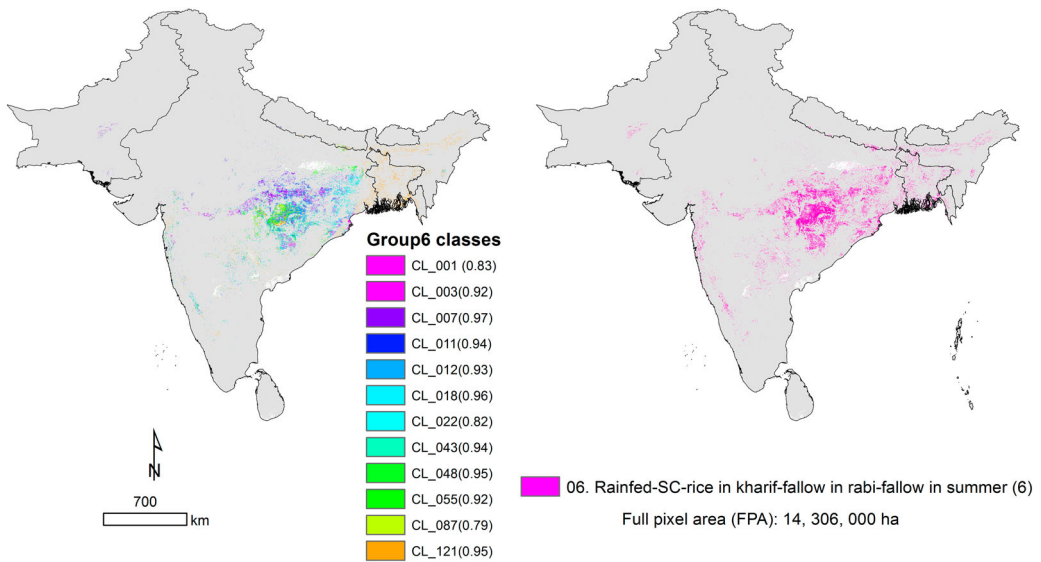


Figure 6. Spatial distribution of rice-fallow classes of rainfed areas. These 12 classes (left image) have rice crop grown during *kharif* (June–October) season, but are left fallow during the *rabi* (November–February) season. The image on the right is the 12 classes merged into a single rice-fallow class.

approach as above, each of the 160 classes of South Asia were grouped into distinct categories, identified, and labeled.

The process, led to reducing 160 class spectral classes (Section 2.6) to 11 combined classes (Figure 8). Of these 11 combined classes, 10 classes were croplands (Figure 8, Table 4). The remainder of the individual non-cropland classes were grouped into a single class (class 11 in Figure 8). Statistics were only provided for the 10 cropland classes (Table 4).

2.8. Identifying croplands with potential for cultivating chickpea (*Cicer arietinum*)

Each of the 10 cropland classes in Figure 8 was assessed (Table 3) for their potential for cultivating grain legumes such as chickpea (*Cicer arietinum*), black gram (*Vigna mungo*), green gram (*Vigna radiata*), and lentil (*Lens culinaris*). Using class 6 as an example, Figure 7 illustrates how the NDVI gradually goes up during mid-July and reaches a peak (0.7) in October and gradually falls to pre-planting levels of about 0.4 indicating the cultivation of *kharif* rice followed by cropland fallow. The dates of vegetation transitions were determined using the NDVI time series and a double-logistic model of vegetation phenology (Biggs et al. 2006; Fischer 1994):

$$\text{NDVI}_t = v_s + \frac{k}{1 + \exp(-c(t-p))} - \frac{k + v_s - v_e}{1 + \exp(-d(t-q))}, \quad (2)$$

where v_s is starting of rice growing season, v_e is the ending of the rice growing season, k is an asymptotic maximum value of NDVI, c and d are the slopes of the NDVI time series at the inflection points, and p and q are the dates of the inflection points (Figure 7).

Class 6 (Figures 4 and 5) is therefore a cropland class that is rainfed during the *kharif* season with rice crop but left fallow in *rabi* seasons and during summer months. Each of the 10 classes in Figure 4 can be characterized and assessed (Table 3) for their potential for cultivating grain legumes. Within these classes, our goal is to identify fallow croplands during *rabi* season. Suitable classes should meet all of the following conditions:

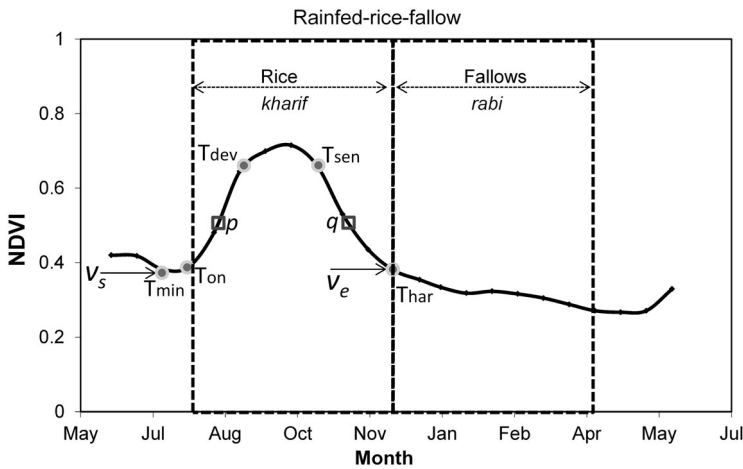


Figure 7. Classic case of rainfed *rabi*-fallow. A model of vegetation phenology and transition dates, as in Equation (3). T_{min} defines the beginning of the time series, T_{on} is onset of greenness, T_{dev} beginning of development stage, T_{sen} onset of senescence, and T_{har} is harvesting time. p and q are the inflection points. Figure shows the progression of class 6. Rainfed, single crop during *kharif* (June–October), fallow during *rabi* (November–February), and fallow during summer (March–May). In this study we want to map rice croplands areas (either in *kharif* or summer) that are left fallow during *rabi*.

- (A) The class should be a fallow cropland during the *rabi* season;
- (B) The class should be a cropland with rice cultivation during *kharif* season; and
- (C) The class should have sufficient moisture/water during the *rabi* season to grow short-season (≤ 3 month), low water-consuming crop determined based on field surveys or expert opinion.

If all of the above conditions are met, then the class (Table 3, Figure 8) becomes suitable for cultivating grain legumes such as chickpea. Each of the 10 classes (Figure 8, Table 3) were analyzed to ascertain if they met the three conditions. The rationale for which classes qualify for grain legume cultivation are given in Table 3.

It is clear that class 1 and class 6 have *fallow croplands* during the *rabi* season. These are also classes where rice is grown in the *kharif* season under rainfed and irrigated conditions. Field surveys and expert opinion gathered during extensive field visits and discussions with local experts also clearly indicated that these two classes have adequate moisture for about three months in the *rabi* season (November–February). Thus they were identified as active croplands that are fallow during *rabi*, but which also have sufficient moisture to grow a short-season (~ 3 month) crop. The rest of the classes do not qualify for *rabi*-season chickpea cultivation since they do not meet one or more criteria mentioned above.

2.9. Calculating sub-pixel areas

Full-pixel areas (FPAs) are not a correct representation of actual areas of crops grown due to obvious sensor resolution issues. Sub-pixel areas (SPAs) or actual area calculation is of greater significance as pixel sizes become coarser. In this study, MOD13Q1 pixels cover 250 m on each side and its area is 6.25 ha. So, for example, for a pixel with only 50% cropped, a FPA-based area calculation per pixel will be 6.25 ha, whereas the SPA or actual area will be 3.125 ha ($6.25 \text{ ha} \times 0.5$). Therefore, areas must be calculated based on SPAs to avoid discrepancies in estimates of cropped area.

Cropland area fractions (CAFs) were calculated for the *kharif* season (June–October) and *rabi* season (November–February) using the methodology described by Thenkabail et al. (2007) and Thenkabail, Schull, and Turrall (2005). This resulted in CAFs that varied between 77.1% or 0.771 for class 10 during *kharif* (June–October) to 97.1% or 0.971 during *kharif* for class 5 (Table 4). In

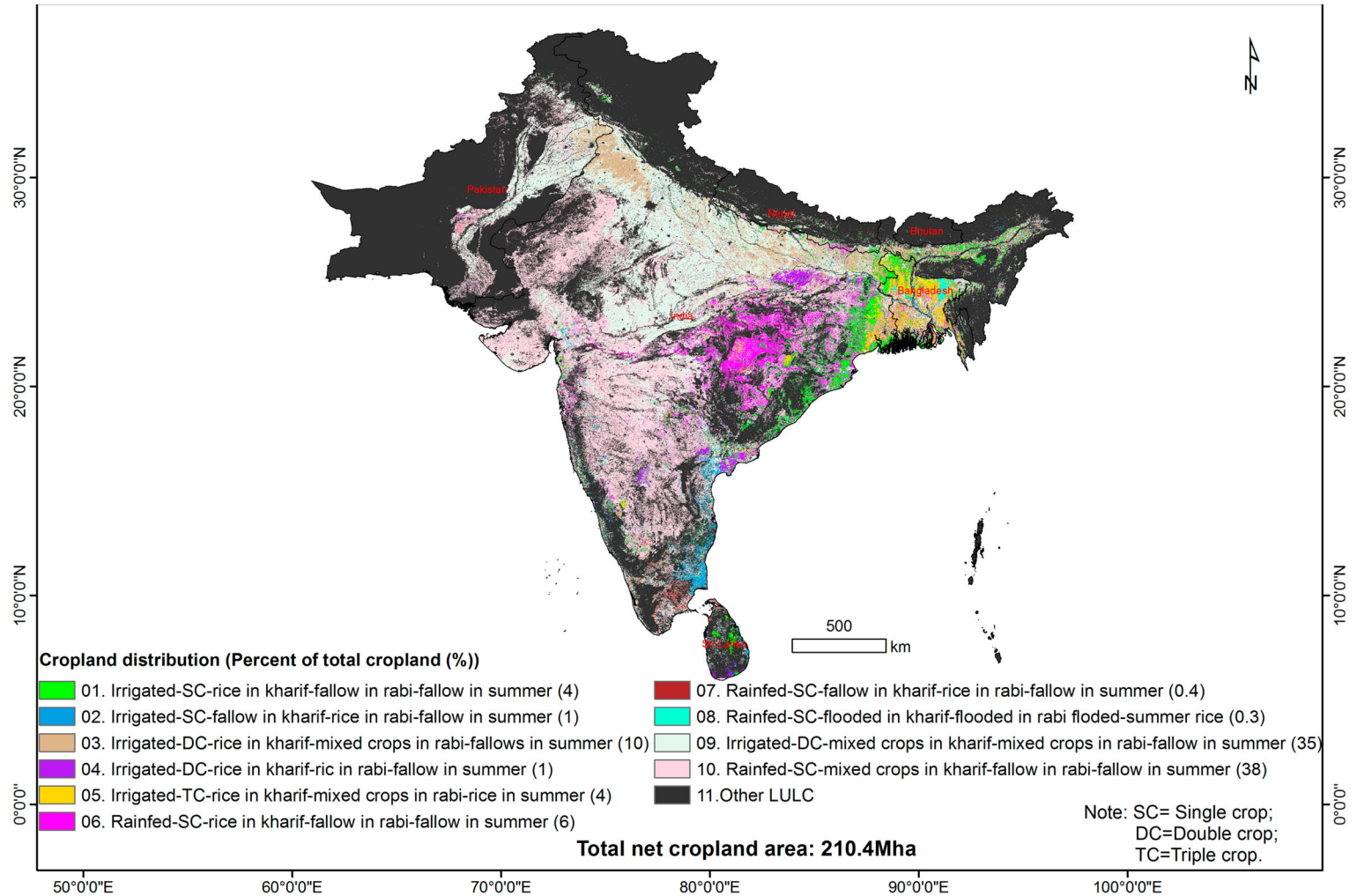


Figure 8. Spatial distribution of croplands and their characteristics in South Asia. The first 10 classes show irrigated or rainfed classes that have single or double or triple cropping and where rice or other crops dominate. The classes also show seasonality of cropping and when croplands are left fallow. Class 11 is non-croplands within the cropland mask. The black areas are non-croplands outside the cropland mask.

seasons when there is little or no crop (cropland fallow), the CAFs were negligible ($\leq 5\%$). The CAFs were calculated for each season using the same procedure as described in detail by Thenkabail et al. (2007). This resulted in calculating SPAs also for each season (Table 4). SPAs are important because we defined a particular class as croplands when, for example, $\geq 50\%$ of the pixel area is cropped. That would mean, a pixel whether it has 50% area cropped or 100% area cropped is still mapped as croplands. In order to get actual areas, FPA needs to be multiplied by CAF (Table 4). Overall, the actual areas are equivalent to SPAs. That is, each pixel in each class is assessed for its actual area as follows:

$$\text{SPAs or actual areas} = \text{FPAs} \times \text{CAFs}$$

Table 4. Cropland statistics of *rice-fallow* (classes 1 and 6) and other classes. Rice systems in South Asia, including other agriculture areas with irrigation source. The table shows full-pixel area (FPA), crop area fraction (CAF), and sub-pixel area (SPA) or actual area. SPA = FPA \times CAF.

Class description	Full-pixel area (FPA) (000'ha)	% of total area (FPA)	Cropland area fractions (CAFs) (%)			Actual cropland area (000'ha)			
			<i>Kharif</i>	<i>Rabi</i>	Summer	<i>Kharif</i>	<i>Rabi</i>	Summer	Total gross crop land area (000'ha)
01. Irrigated-SC-rice in <i>kharif</i>-fallow in <i>rabi</i>-fallow in summer	10,273	4.9	96.1	3.1	3.2	9873	318	329	10,520
02. Irrigated-SC-fallow in <i>kharif</i> -rice in <i>rabi</i> -fallow in summer	2952	1.4	3.1	92.2	3.1	92	2722	92	2905
03. Irrigated-DC-rice in <i>kharif</i> -mixed crops in <i>rabi</i> -fallow in summer	20,811	9.9	94	88.9	3.3	19,562	18,501	687	38,750
04. Irrigated-DC-rice in <i>kharif</i> -rice in <i>rabi</i> -fallow in summer	2,801	1.3	96.3	94.6	3	2698	2650	84	5432
05. Irrigated-TC-rice in <i>kharif</i> -mixed crops in <i>rabi</i> -rice in summer	5,726	2.7	97.3	91.7	89.8	5571	5250	5142	15,963
06. Rainfed-SC-rice in <i>kharif</i>-fallow in <i>rabi</i>-fallow in summer	14,306	6.8	91.3	2.9	2.1	13,061	415	300	13,777
07. Rainfed-SC-fallow in <i>kharif</i> -rice in <i>rabi</i> -fallow in summer	891	0.4	3	93.6	3	27	834	27	888
08. Rainfed-SC-flooded in <i>kharif</i> -flooded in <i>rabi</i> flooded-summer rice	618	0.3	3	3	91.9	19	19	568	605
09. Irrigated-DC-mixed crops in <i>kharif</i> -mixed crops in <i>rabi</i> -fallow in summer	73,633	35.0	86.7	83.2	3.5	63,840	61,263	2577	127,680
10. Rainfed-SC-mixed crops in <i>kharif</i> -fallow in <i>rabi</i> -fallow in summer	78,416	37.3	77.7	18	0	60,929	14,115	0	75,044
Total croplands	210,428					175,671	106,087	9805	291,563

Note: Net cropland areas cultivated in South Asia, full-pixel areas (FPA) = 210,428,000 ha.

Net cropland areas cultivated in South Asia, sub-pixel areas (SPAs) or actual areas during summer season (March–May) = 9,805,241 ha.

Gross cropland areas cultivated in South Asia, sub-pixel areas (SPAs) or actual areas = 291,562,500 ha.

For classes 1 and 6 (Note: these two classes have rice during *kharif* and left fallow in *rabi*).

Total net cultivated areas during *kharif* in South Asia, SPAs or actual areas of classes 1 and 6 = 22,933,730 ha.

Total net cultivated areas during *rabi* in South Asia, SPAs or actual areas of classes 1 and 6 = 733,343 ha.

Total uncultivated areas during *rabi* that were cultivated during *kharif*, SPAs or actual areas of classes 1 and 6 = 22,200,576 ha.

2.10. Accuracy assessments and comparison with national statistics

Accuracy assessment was based on a total of 568 independent ground samplings, as described in Section 2.4. These ground samples were not used in class identification and labeling and hence are completely independent. The accuracy assessment is performed using an error matrix (Congalton 1991). The columns (x -axis) of an error matrix contain the ground survey data samples and the rows (y -axis) represent the results of the classified rice maps. The error matrix is a multi-dimensional table in which the cells contain changes from one class to another. The statistical approach of accuracy assessment consists of different multi-variate statistical analyses. A frequently used measure is kappa, which is designed to compare results from different regions or different classifications (Congalton 1991).

The SPAs were calculated at district level administrative units and compared with national statistics at the district level (e.g. www.indiastat.com) (INDIASTAT 2015). Statistics for India were obtained from the website of the Ministry of Agriculture's Directorate of Rice Development (<http://dacnet.nic.in/rice/>), while statistics for Bangladesh, Nepal, Pakistan, Nepal, and Bhutan were obtained from national statistical departments (BBS 2011; CBS 2013; SDCS 2013). Based on the data available from the target countries, we compared irrigated area statistics derived using MODIS data gathered at the provincial or state level were compared, resulting in 62 administrative units. Similarly, rice cropland estimates derived from MODIS data analysis were compared at the sub-district level (812 administrative units).

3. Results

Considering the objectives of this study and based on the methods described in section 2.0 and its sub-sections, distinct cropland classes of South Asia were mapped (Figure 8). The characteristics of these cropland classes were then used to determine *fallow croplands* during the *rabi* season that are suitable areas for cultivating grain legumes (Figure 9, Table 4).

3.1. Spatial distribution of croplands in south Asia

The spatial distribution of cropland areas of South Asia with 10 distinct cropland classes and an 11th other land cover/land use (LCLU) is shown in Figure 8, with statistics provided in Table 4.

Based on the FPA, 44% (210.4 Mha) of the total geographic area (477 Mha) of South Asia was under croplands (classes 1 to 10 in Figure 8, Table 4). Of the 210.4 Mha, class 9 (irrigated-DC-mixed crops in *kharif*-mixed crops in *rabi*-fallow in summer) with 35% and class 10 (rainfed-SC-mixed crops in *kharif*-fallow in *rabi*-fallow in summer) with 37.3% dominate. Even though these are large areas, class 9 is irrigated and cultivated in *rabi* as well as *kharif*, whereas class 10 is rainfed and is cultivated only in *kharif*. Although during the *rabi* season class 10 is fallow, cultivation of crops is not viable since these lands are rainfed during *kharif* and do not have sufficient residual moisture for crop growth during the *rabi* season. The NDVI phenological characteristics of these classes are shown in Figure 4. All 10 cropland classes are mapped (Figure 4) and their actual areas (or SPAs) are established (Table 4).

The FPA of croplands in South Asia was 210.48 Mha (Figure 9, Table 4). Of this, 175.67 Mha (83% of net cropped area) is SPAs during *kharif* (Table 4). This significantly differs from the *rabi* crop land area that is estimated at about 50% of the net cropped area. While classes 9 and 10, due to their large area, dominate the *kharif* season, only class 9 dominates during the *rabi* season, followed by class 3, indicating the importance of irrigation for growing a *rabi* crop.

3.2. Cropland classes with *rabi*-fallow suitable for cultivating grain legumes across South Asia

Of the 10 cropland classes (Figure 8, Table 4), two classes (Figure 9) meet the three critical criterion for being eligible for *rabi*-season cropping. There two classes were: irrigated-SC-rice in *kharif*-fallow

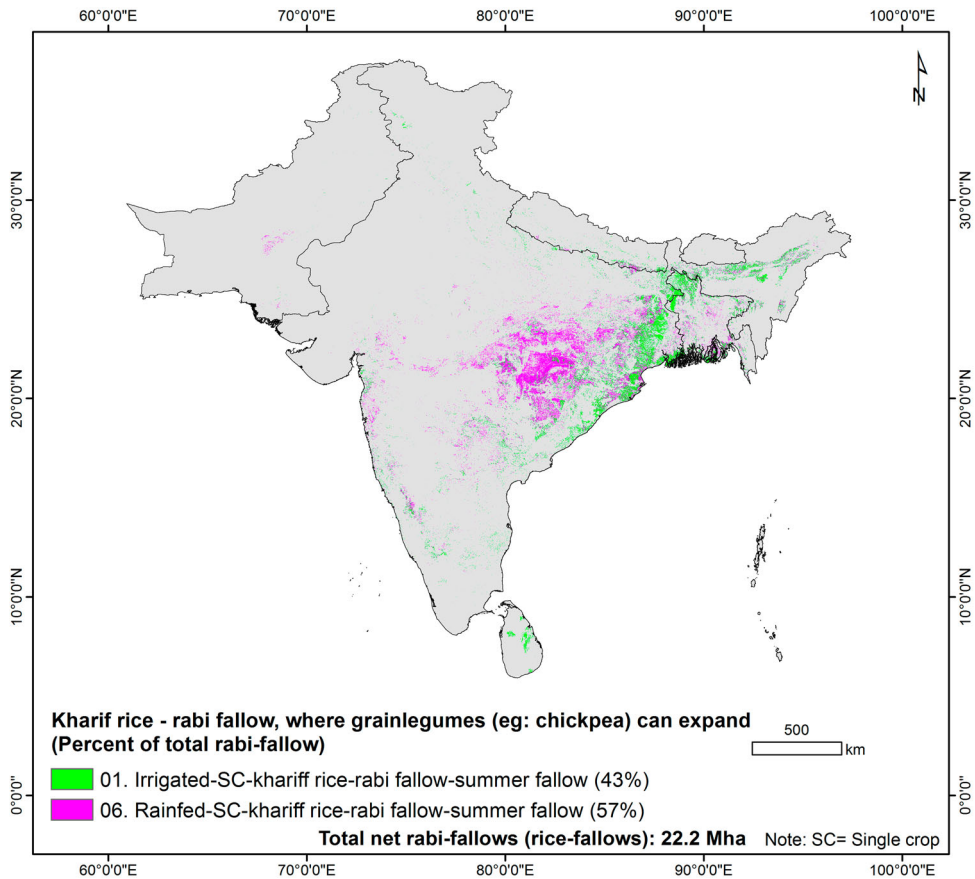


Figure 9. Rice-fallow of South Asia. Two cropland classes where rice is grown during *kharif* (June–October) season, but are fallow croplands during *rabi* (November–February) season are shown here. Class 1 has irrigated rice crop during in *kharif* season, and class 6 has rainfed rice during *kharif* season. Both classes are left fallow during the *rabi* season. The total areas of such rice-fallow is 22.2 Mha where second or *rabi*-season, low water-consuming, short-season (≤ 3 month) legume crops such as chickpea, black gram, green gram, and lentils can be grown.

in *rabi*-fallow in summer (class 1); and rainfed-SC-rice in *kharif*-fallow in *rabi*-fallow in summer (class 6). These classes are rice-fallow areas because rice is grown in these class areas during *kharif* and overwhelmingly left fallow during *rabi*.

The total net cultivated area during *kharif* in South Asia, SPAs or actual areas, of classes 1 and 6 were 22.93 Mha (Table 4). The total net cultivated area during *rabi* in South Asia, SPAs or actual areas, of classes 1 and 6 were 0.73 Mha (Table 4). Therefore this leaves a total uncultivated area (*fallow croplands*) of 22.2 Mha (22.93–0.73 Mha) during *rabi* from classes 1 and 6 (Table 4) and potentially available for *rabi*-season cropping.

3.3. Accuracies and errors

Accuracies of the classes were established based on 568 ground sample data (Table 5). This provided an overall accuracy of 82% with kappa of 0.79. The user's and producer's accuracies of most classes were above 80%. Even when they were somewhat lower, the class mix is mainly among cropland classes. Classes 1 and 6 are cropland fallow classes and hence critical to this study. These classes were determined to have producer's accuracy of 80% and 75%, respectively, while the user's accuracy of 82% and 69%, respectively. The lower accuracies for some of the classes can be improved through

Table 5. Accuracy assessments using error matrix. Accuracies and errors of cropland classes including *rice-fallow* classes of South Asia).

Crop classification	01.	02.	03.	04.	05.	06.	07	08	09.	10.	11.	Class totals	Reference totals	Classified totals	Users' accuracy (%)	Producers' accuracy (%)	Kappa
01. Irrigated-SC-rice in <i>kharif</i> -fallow in <i>rabi</i> -fallow in summer	37	0	0	1	1	6	0	0	1	0	0	45	46	37	82	80	0.8
02. Irrigated-SC-fallow in <i>kharif</i> -rice in <i>rabi</i> -fallow in summer	0	19	0	1	3	0	1	1	1	0	0	21	26	19	90	73	0.7
03. Irrigated-DC-rice in <i>kharif</i> -mixed crops in <i>rabi</i> -fallow in summer	0	0	37	1	6	1	1	0	2	0	0	40	48	37	93	77	0.8
04. Irrigated-DC-rice in <i>kharif</i> -rice in <i>rabi</i> -fallow in summer	0	0	0	49	1	1	0	0	2	1	1	58	55	49	84	89	0.9
05. Irrigated-TC-rice in <i>kharif</i> -mixed crops in <i>rabi</i> -rice in summer	0	0	1	0	54	0	1	0	4	0	0	74	60	54	73	90	0.9
06. Rainfed-SC-rice in <i>kharif</i> -fallow in <i>rabi</i> -fallow in summer	6	1	0	1	4	43	0	0	0	2	0	62	57	43	70	75	0.7
07. Rainfed-SC-fallow in <i>kharif</i> -rice in <i>rabi</i> -fallow in summer	0	0	0	2	2	0	5	0	0	0	1	12	10	5	42	50	0.5
08. Rainfed-SC-flooded in <i>kharif</i> -flooded in <i>rabi</i> flooded-summer rice	0	0	0	0	0	0	0	5	0	0	0	7	5	5	71	100	1
09. Irrigated-DC-mixed crops in <i>kharif</i> -mixed crops in <i>rabi</i> -fallow in summer	0	1	1	3	2	10	2	1	88	5	2	102	115	88	86	77	0.7
10. Rainfed-SC-mixed crops in <i>kharif</i> -fallow in <i>rabi</i> -fallow in summer	2	0	1	0	0	0	1	0	0	105	0	122	109	105	86	96	1
11. Other LULC	0	0	0	0	1	1	1	0	4	9	21	25	37	21	84	57	0.5
Column Total	45	21	40	58	74	62	12	7	102	122	25	568	568	463			

Note: Overall classification accuracy = 82%; overall kappa statistics = 0.79; X-axis is Ground survey information and Y-axis is Modis derived classification.

a number of measures that include: (a) access to greater number of reference/training data, (b) conducting more regional analysis and/or analyzing them by AEZs, (c) incorporating other data such as slope, soils, and elevation, (d) aggregating classes where areas are very small (e.g. small classes like 7 and 8 with a large class like 6 to get broader rainfed group), and (e) incorporating higher resolution time-series remote sensing data such as Landsat 30 m every 16-day.

3.4. Comparison with district-wise cropland statistics

Figure 6 illustrates the spatial extent of rice growing areas or *rice-fallow* (Table 5) where rice crop is grown during the *kharif* (June–October) and left fallow during *rabi* (November–February). In order to assess how well the spatial extent of rice fallow were estimated, we correlated (Figures 10 and 11) district-wise statistics of rice areas of *kharif* derived from remote sensing in this study with the statistics obtained from national systems; resulting in a R^2 value of 0.84. Some of the uncertainty that we see in Figure 10 is as a result of the uncertainties existing in the national statistics. Figure 11 shows district by district correlation map between the MODIS derived areas versus the district statistics from the national systems. Correlations are high (0.8 or greater) in districts where rice is dominant crop. Low correlations are in areas where there is fragmentation in rice growing areas.

4. Discussion

Mapping rice-fallow (Figure 9, Table 4) is useful for providing intensification options for producing more food, which is critical for ensuring the global food security. Greater food production for a growing population requires more land. Since cropland expansion is not feasible and has costly environmental and ecological impacts (Kuemmerle et al. 2013; Thenkabail et al. 2012; Tilman 1999; Tilman et al. 2002), cropland intensification by cultivating existing fallow croplands is a possible option. In certain parts of South Asia, croplands are left fallow over large areas during the *rabi* season (November–February) (Figures 6 and 9). The areas where rice crop is grown during the *kharif*

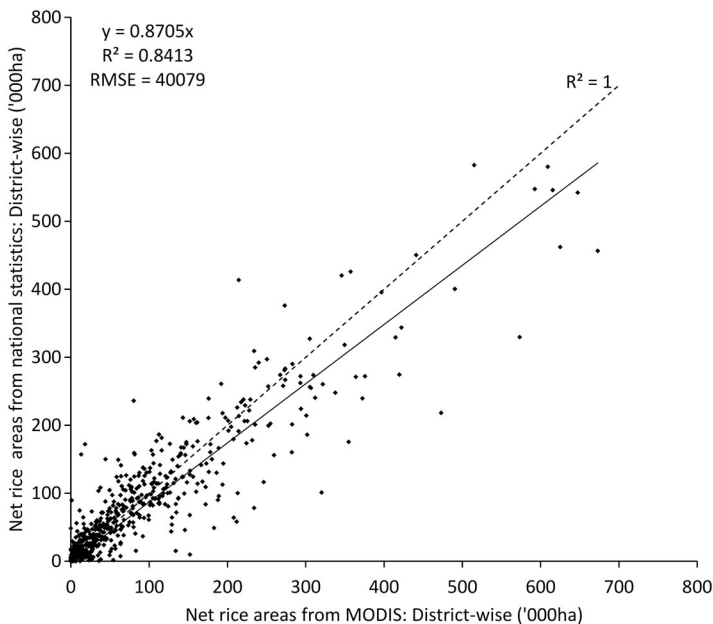


Figure 10. Remote-sensing-derived rice area comparisons with national statistics. The district-wise rice areas derived using MODIS 250 m are compared with agricultural census data for 2010–11.

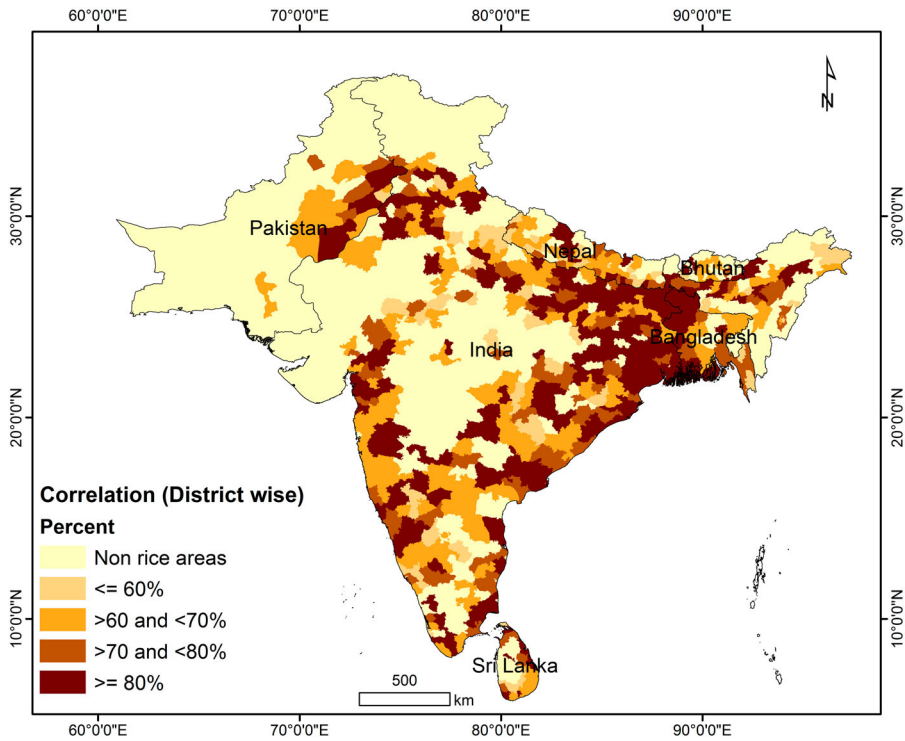


Figure 11. Correlation between MODIS derived *kharif* rice areas versus the national statistics.

season (June–October) also hold significant moisture/water during the *rabi* season to sustain a short-season, low water-consuming grain legume crop such as chickpea. This study extensively investigated South Asia using MODIS 250 m NDVI time series to arrive at cropland classes (Figure 8) from which two cropland fallow classes (Figure 10) were identified as most suitable areas for the *rabi*-season cultivation with short-season, low water-consuming grain legumes. These two classes have a total area of about 22.2 Mha (Table 4, Figure 9) as fallow croplands during the *rabi* season.

The present research used MOD13Q1.5 temporal data to identify rice-fallow with rice systems and irrigated areas across South Asia. MODIS captures imagery on a daily basis. The 16-day composites from the daily acquisitions combine to make a time-series dataset over a crop year or a calendar year. This type of dataset provides temporal profiles of crop growing locations to identify the start of season, peak growth stage, and harvest date during each season. The value of NDVI as function of time also helps in identifying the type of crop in an eco-region based on certain peak thresholds for that crop. This study applies an SMT which is found to be ideal in mapping irrigated and rainfed areas (Thenkabail et al. 2007) and mapping rice areas (Gumma et al. 2011a). Mapping the spatial distribution of *rice-fallow* areas using MODIS 250 m 16-day time series and ground survey information with SMTs is a significant new advancement in the use of this technology. The advantage of using an SMT in this study is in ability to selectively use the ideal spectral profiles of rice during the rainy season. The rainfed rice spectral class varies from 0.25 to 0.70 for purely rainfed rice and 0.25 to 0.85 for irrigated rice during the rainy season. The qualitative (shape) difference between ideal spectra and class spectra is narrow and represents the fallow lands accurately.

SMT is a powerful concept (Homayouni and Roux 2003; Thenkabail et al. 2007) for mapping croplands or for that matter any land use/land cover (LULC) using time-series remotely sensed data. The process of matching class spectra with ideal spectra will be invaluable in fast and automatic identification and labeling of classes. However, SMTs will not work without accurate ground data/

Table 6. Rice-fallow by country. Country-wise distribution of areas of *rabi-rice-fallow* in South Asia.

Country	Area in (000'ha)		Total
	01. Irrigated-SC-rice in <i>kharif</i> -fallow in summer	06. Rainfed-SC-rice in <i>kharif</i> -fallow in summer	
Bangladesh	1190	739	1929
Bhutan	3	1	4
India	7909	11,695	19,604
Nepal	194	117	311
Pakistan	14	93	107
Sri Lanka	244	1	245
Total	9554	12,646	22,200

knowledge that help develop accurate sets of ideal spectral libraries. Uncertainties and/or inaccuracies in ground data will result in class labeling errors leading to uncertainties in classes that are interpreted and mapped.

Cropped area fractions were calculated to better calibrate the MODIS pixel area to the real irrigated/rice or rainfed/rice area. Also, this method relies on ground survey information that is a truly representative sample of the fragmented rice systems. Higher resolution imagery could be used to provide a more accurate estimate of pure classes, but wall to wall coverage, repeat coverage during crop growing period, costs, and massive processing are all major issues hard to surmount for such large areas as South Asia. Results clearly show that present methods and MODIS time-series data have many advantages such as capturing large-scale cropping pattern. But to minimize errors, additional research will be attempted with multi-sensor images, including Landsat 30-m data with advanced fusion techniques (Gumma et al. 2011b).

Source of water and crop intensity are also considered in the classification of land cover. The potential areas among these rice-based systems are classes 1 and 6 with an extent of around 22.2 Mha (Table 6). The land use class 10 is another potential area where the *rabi*-fallow are very high (47 Mha), but the suitability for legume production needs to be assessed. Also, crop modeling tools can help in assessing the potential yields in classes 1 and 6, but class 10 needs a thorough investigation of the edapho-climatic suitability. The largest rice-fallow area under class 6 is in the north-eastern plateau of India, including Chattisgarh, Chotanagpur Plateau and the Assam region, which are under red and yellow soils. The important states in India where the rice-fallow areas can be exploited are Chattisgarh, Odisha, West Bengal, Madhya Pradesh, Telangana, Assam and Maharashtra. The Barind Tract (Rajshahi, Naogadh, Bogra, and Dinajpur divisions) in Bangladesh is a potential region based on the eco-physiography covering an area of 2 Mha. In Nepal the eastern and central *terai* regions with an extent of 0.3 Mha are the potential areas. Sri Lanka is another potential country with an area of 0.26 Mha spread over the central, north-central, and eastern regions. The Sind region in Pakistan has the largest rice-fallow area with about 0.09 Mha specifically in the Sulaiman Piedmont.

5. Conclusions

The study developed maps of *rice-fallow* cropland areas, where rice grown during the *kharif* season (June–October) but left fallow during the *rabi* season (November–February), for entire South Asia based on MODIS 250 m every 16-day NDVI time-series data analyzed using SMTs. These *rice-fallow* cropland areas can support low water-consuming, short-growing season (≤ 3 months) *rabi*-season legumes such as chickpea, black gram, green gram, and lentils, but are unsuitable for growing rice crop or other cereals during the *rabi* season due to lack of moisture/water to sustain these high water-consuming, relatively long-growing season (> 3 month) crops. In South Asia, the *rice-fallow* cropland area classes occupied 22.2 Mha (Figure 9, Table 4) of SPAs or actual areas during the *kharif* season. Currently, out of the 22.2 Mha of actual areas identified during the *kharif* season, only about

0.77 Mha is cropped during the *rabi* season. This has left a massive 21.43 Mha of *fallow* cropland areas available to grow short duration, low water-consuming legume crops during the *rabi* after monsoon *kharif* rice cultivation in these areas. The overall accuracy of cropland mapping was 82% with kappa coefficient of 0.79. The *rabi*-fallow cropland classes (with rice as *kharif* crop) showed producer's accuracies between 75% and 80% and user's accuracies between 69% and 82%. Thus, this study has demonstrated the use of remote-sensing data and techniques to identify and map *rice-fallow* cropland areas in South Asia, with the overall goal of providing baseline information to policy and resource planning for sustainable development of production agriculture through cropland intensification and diversification rather than cropland area expansion for meeting the food and nutritional demands of growing population that is also economically advancing.

Acknowledgments

Authors would like thank to International Rice Research Institute (IRRI) for providing ground survey data and district-wise national statistics; Dr Dheeravath Venkateshwarlu, Dr Andrew Nelson, and Dr Mitch Scull for supporting ground surveys in India; Dr Saidul Islam for Bangladesh ground survey data; Dr Nimal Desanayake for Sri Lanka ground survey data.

Funding

This research was supported by two CGIAR Research Programs: Dryland Cereals, Grain legumes and WLE. The research was also supported by the global food security support analysis data at 30 m project (GFSAD30; <http://geography.wr.usgs.gov/science/croplands/>; <https://croplands.org/>) funded by the NASA MEaSURES [grant number: NNH13AV82I] (Making Earth System Data Records for Use in Research Environments) funding obtained through NASA ROSES solicitation as well as by the Land Change Science (LCS), Land Remote Sensing (LRS), and Climate Land Use Change Mission Area Programs of the U.S. Geological Survey (USGS).

ORCID

Murali Krishna Gumma  <http://orcid.org/0000-0002-3760-3935>

References

- Alexandratos, N., and J. Bruinsma. 2012. World Agriculture Towards 2030/2050: The 2012 Revision. ESA Work. Pap 3. Accessed June 8, 2015. <http://large.stanford.edu/courses/2014/ph240/yuan2/docs/ap106e.pdf>.
- Anderson, W., L. You, S. Wood, U. Sichra, and W. Wu. 2015. "An Analysis of Methodological and Spatial Differences in Global Cropping Systems Models and Maps." *Global Ecology and Biogeography* 24: 180–191.
- Badhwar, G. D. 1984. "Automatic Corn–Soybean Classification Using Landsat MSS Data. I. Near-harvest Crop Proportion Estimation." *Remote Sensing of Environment* 14: 15–29.
- Bantilan, C., D. K. Charyulu, P. Gaur, M. S. Davala, and J. Davis. *Forthcoming*. *Short Duration Chickpea Technology: Enabling Legumes Revolution in Andhra Pradesh*. Hyderabad: ICRISAT, Patancheru.
- BBS. 2011. Hand book of agriculture statistics, Bangladesh Bureau of Statistics. Accessed January 20, 2012. <http://www.bbs.gov.bd/webtestapplication/userfiles/image/AgricultureCensus/>.
- Biggs, T. W., P. S. Thenkabail, M. K. Gumma, C. A. Scott, G. R. Parthasaradhi, and H. N. Turrall. 2006. "Irrigated Area Mapping in Heterogeneous Landscapes with MODIS Time Series, Ground Truth and Census Data, Krishna Basin, India." *International Journal of Remote Sensing* 27: 4245–4266.
- Biradar, C. M., P. S. Thenkabail, P. Noojipady, Y. Li, V. Dheeravath, H. Turrall, M. Velpuri, et al. 2009. "A Global Map of Rainfed Cropland Areas (GMRC) at the End of Last Millennium Using Remote Sensing." *International Journal of Applied Earth Observation and Geoinformation* 11: 114–129.
- CBS. 2013. Central Bureau of Statistics: Statistical Year Book of Nepal – 2013. Accessed August 21, 2015. <http://cbs.gov.np/>.
- Cihlar, J., Q. Xiao, J. Chen, J. Beaubien, K. Fung, and R. Latifovic. 1998. "Classification by Progressive Generalization: A New Automated Methodology for Remote Sensing Multichannel Data." *International Journal of Remote Sensing* 19: 2685–2704.
- Congalton, R. G. 1991. "A Review of Assessing the Accuracy of Classifications of Remotely Sensed Data." *Remote Sensing of Environment* 37: 35–46.

- Dabin, Z., Y. Pengwei, Z. Na, Y. Changwei, C. Weidong, and G. Yajun. 2016. "Contribution of Green Manure Legumes to Nitrogen Dynamics in Traditional Winter Wheat Cropping System in the Loess Plateau of China." *European Journal of Agronomy* 72: 47–55.
- Dheeravath, V., P. S. Thenkabail, G. Chandrakantha, P. Noojipady, G. P. O. Reddy, C. M. Biradar, M. K. Gumma, and M. Velpuri. 2010. "Irrigated areas of India Derived Using MODIS 500 m Time Series for the Years 2001–2003." *ISPRS Journal of Photogrammetry and Remote Sensing* 65: 42–59.
- Dixon, J., A. M. Omwega, S. Friel, C. Burns, K. Donati, and R. Carlisle. 2007. "The Health Equity Dimensions of Urban Food Systems." *Journal of Urban Health* 84: 118–129.
- FAO. 2015. FAOSTAT. Accessed June 2, 2015. <http://faostat.fao.org/>.
- FAO-IIASA. 2012. Global Agro-ecological Zones (GAEZ v3.0). IIASA and FAO. Accessed November 28, 2015. <http://webarchive.iiasa.ac.at/Research/LUC/GAEZv3.0/>.
- Fischer, A. 1994. "A Model for the Seasonal Variations of Vegetation Indices in Coarse Resolution Data and its Inversion to Extract Crop Parameters." *Remote Sensing of Environment* 48: 220–230.
- Foerster, S., K. Kaden, M. Foerster, and S. Itzerott. 2012. "Crop Type Mapping Using Spectral–temporal Profiles and Phenological Information." *Computers and Electronics in Agriculture* 89: 30–40.
- Foley, J. A., N. Ramankutty, K. A. Brauman, E. S. Cassidy, J. S. Gerber, M. Johnston, N. D. Mueller, C. O'Connell, D. K. Ray, and P. C. West. 2011. "Solutions for a Cultivated Planet." *Nature* 478: 337–342.
- Garnett, T., M. Appleby, A. Balmford, I. Bateman, T. Benton, P. Bloomer, B. Burlingame, M. Dawkins, L. Dolan, and D. Fraser. 2013. "Sustainable Intensification in Agriculture: Premises and Policies." *Science* 341: 33–34.
- Ghosh, P., K. Bandyopadhyay, R. Wanjari, M. Manna, A. Misra, M. Mohanty, and A. S. Rao. 2007. "Legume Effect for Enhancing Productivity and Nutrient Use-efficiency in Major Cropping Systems – An Indian Perspective: A Review." *Journal of Sustainable Agriculture* 30: 59–86.
- Gray, J., M. Friedl, S. Frolking, N. Ramankutty, A. Nelson, and M. Gumma. 2014. "Mapping Asian Cropping Intensity with MODIS." *IEEE Journal of Selected Topics in Applied Earth Observations and Remote Sensing* 7 (8): 3373–3379. doi:10.1109/JSTARS.2014.2344630.
- Gumma, M. K., K. Kajisa, I. A. Mohammed, A. M. Whitbread, A. Nelson, A. Rala, and K. Palanisami. 2015a. "Temporal Change in Land Use by Irrigation Source in Tamil Nadu and Management Implications." *Environmental Monitoring and Assessment* 187: 1–17.
- Gumma, M. K., S. Mohanty, A. Nelson, R. Arnel, I. A. Mohammed, and S. R. Das. 2015b. "Remote Sensing Based Change Analysis of Rice Environments in Odisha, India." *Journal of Environmental Management* 148: 31–41.
- Gumma, M. K., A. Nelson, P. S. Thenkabail, and A. N. Singh. 2011a. "Mapping Rice Areas of South Asia Using MODIS Multitemporal Data." *Journal of Applied Remote Sensing* 5: 053547. doi:10.1117/1.3619838.
- Gumma, M. K., P. S. Thenkabail, F. Hideto, A. Nelson, V. Dheeravath, D. Busia, and A. Rala. 2011b. "Mapping Irrigated Areas of Ghana Using Fusion of 30 m and 250 m Resolution Remote-Sensing Data." *Remote Sensing* 3: 816–835.
- Gumma, M. K., P. S. Thenkabail, A. Maunahan, S. Islam, and A. Nelson. 2014. "Mapping Seasonal Rice Cropland Extent and Area in the High Cropping Intensity Environment of Bangladesh Using MODIS 500 m Data for the Year 2010." *ISPRS Journal of Photogrammetry and Remote Sensing* 91: 98–113.
- Gumma, M. K., P. S. Thenkabail, I. V. Muralikrishna, M. N. Velpuri, P. T. Gangadhararao, V. Dheeravath, C. M. Biradar, S. Acharya Nalan, and A. Gaur. 2011c. "Changes in Agricultural Cropland Areas Between a Water-surplus Year and a Water-deficit Year Impacting Food Security, Determined Using MODIS 250 m Time-series Data and Spectral Matching Techniques, in the Krishna River Basin (India)." *International Journal of Remote Sensing* 32: 3495–3520.
- Hobbs, P., and M. Osmanzai. 2011. "Important Rainfed Farming Systems of South Asia." In *Rainfed Farming Systems*, edited by P. Tow, I. Cooper, I. Partridge, and C. Birch, 603–641. Amsterdam: Springer.
- Homayouni, S., and M. Roux. 2003. "Material Mapping from Hyperspectral Images Using Spectral Matching in Urban Area." In *IEEE Workshop in honour of Prof. Landgrebe*, edited by P. Landgrebe. Washington, DC, USA.
- INDIASTAT. 2015. State-wise Net Area Irrigated by Source in India and State-wise Irrigated Area Under Crops in India. Accessed May 30, 2015. www.indiastat.com.
- Knight, J. F., R. L. Lunetta, J. Ediriwickrema, and S. Khorram. 2006. "Regional Scale Land-Cover Characterization using MODIS-NDVI 250 m Multi-Temporal Imagery: A Phenology Based Approach." *GIScience and Remote Sensing* 43: 1–23.
- Kontgis, C., A. Schneider, and M. Ozdogan. 2015. "Mapping Rice Paddy Extent and Intensification in the Vietnamese Mekong River Delta with Dense Time Stacks of Landsat Data." *Remote Sensing of Environment* 169: 255–269.
- Kuemmerle, T., K. Erb, P. Meyfroidt, D. Müller, P. H. Verburg, S. Estel, H. Haberl, P. Hostert, M. R. Jepsen, and T. Kastner. 2013. "Challenges and Opportunities in Mapping Land Use Intensity Globally." *Current Opinion in Environmental Sustainability* 5: 484–493.
- Lobell, D. B., G. P. Asner, J. I. Ortiz-Monasterio, and T. L. Benning. 2003. "Remote Sensing of Regional Crop Production in the Yaqui Valley, Mexico: Estimates and Uncertainties." *Agriculture, Ecosystems & Environment* 94: 205–220.

- Pittman, K., M. C. Hansen, I. Becker-Reshef, P. V. Potapov, and C. O. Justice. 2010. "Estimating Global Cropland Extent with Multi-year MODIS Data." *Remote Sensing* 2: 1844–1863.
- Sakamoto, T., M. Yokozawa, H. Toritani, M. Shibayama, N. Ishitsuka, and H. Ohno. 2005. "A Crop Phenology Detection Method Using Time-Series MODIS Data." *Remote Sensing of Environment* 96: 366–374.
- Salmon, J. M., M. A. Friedl, S. Frolking, D. Wisser, and E. M. Douglas. 2015. "Global Rain-fed, Irrigated, and Paddy Croplands: A New High Resolution Map Derived from Remote Sensing, Crop Inventories and Climate Data." *International Journal of Applied Earth Observation and Geoinformation* 38: 321–334.
- SDCS. 2013. Sri Lanka Department of Census and Statistics, Agriculture and Environment Statistics Division. Accessed August 21, 2015. <http://www.statistics.gov.lk/agriculture/index.htm>.
- See, L., S. Fritz, L. You, N. Ramankutty, M. Herrero, C. Justice, I. Becker-Reshef, P. Thornton, K. Erb, and P. Gong. 2015. "Improved Global Cropland Data as an Essential Ingredient for Food Security." *Global Food Security* 4: 37–45.
- Settle, W. H., H. Ariawan, E. T. Astuti, W. Cahyana, A. L. Hakim, D. Hindayana, and A. S. Lestari. 1996. "Managing Tropical Rice Pests Through Conservation of Generalist Natural Enemies and Alternative Prey." *Ecology* 77 (7): 1975–1988.
- Subbarao, G., J. Kumar Rao, C. Kumar, U. Johansen, A. Irshad, L. Krishna Rao, K. Venkataratnam, K. Hebbar, M. Sai, and D. Harries. 2001. *Spatial Distribution and Quantification of Rice-fallows in South Asia: Potential for Legumes*. Hyderabad: ICRISAT. 316pp.
- Thenkabail, P. S. 2010. "Global Croplands and their Importance for Water and Food Security in the Twenty-first Century: Towards an Ever Green Revolution that Combines a Second Green Revolution with a Blue Revolution." *Remote Sensing* 2: 2305–2312.
- Thenkabail, P. S., C. M. Biradar, P. Noojipady, V. Dheeravath, Y. Li, M. Velpuri, M. Gumma, et al. 2009b. "Global Irrigated Area Map (GIAM), Derived from Remote Sensing, for the End of the Last Millennium." *International Journal of Remote Sensing* 30: 3679–3733.
- Thenkabail, P., C. Biradar, P. Noojipady, V. Dheeravath, Y. Li, M. Velpuri, M. Gumma, et al. 2009a. "Global Irrigated Area Map (GIAM) for the End of the Last Millennium Derived from Remote Sensing." *International Journal of Remote Sensing* 30 (14): 3679–3733.
- Thenkabail, P. S., C. M. Biradar, P. Noojipady, V. Dheeravath, Y. J. Li, M. Velpuri, G. Reddy, X. Cai, M. Gumma, and H. Turrall. 2008. *A Global Irrigated Area Map (GIAM) Using Remote Sensing at the End of the Last Millennium*. Colombo: International Water Management Institute.
- Thenkabail, P., P. Gangadhara Rao, T. Biggs, M. Gumma, and H. Turrall. 2007. "Spectral Matching Techniques to Determine Historical Land-use/land-cover (LULC) and Irrigated Areas Using Time-series 0.1-Degree AVHRR Pathfinder Datasets." *Photogrammetric Engineering & Remote Sensing* 73: 1029–1040.
- Thenkabail, P. S., J. W. Knox, M. Ozdogan, M. K. Gumma, R. G. Congalton, Z. Wu, C. Milesi, A. Finkral, M. Marshall, and I. Mariotto. 2012. "Assessing Future Risks to Agricultural Productivity, Water Resources and Food Security: How can Remote Sensing Help?." *Photogrammetric Engineering and Remote Sensing* 78: 773–782.
- Thenkabail, P. S., M. Schull, and H. Turrall. 2005. "Ganges and Indus River Basin Land Use/Land Cover (LULC) and Irrigated Area Mapping Using Continuous Streams of MODIS Data." *Remote Sensing of Environment* 95: 317–341.
- Thiruvengadachari, S., and R. Sakthivadivel. 1997. *Satellite Remote Sensing for Assessment of Irrigation System Performance: A Case Study in India. Research Report 9*. Colombo: International Irrigation Management Institute.
- Tilman, D. 1999. "Global Environmental Impacts of Agricultural Expansion: The Need for Sustainable and Efficient Practices." *Proceedings of the National Academy of Sciences* 96: 5995–6000.
- Tilman, D., K. G. Cassman, P. A. Matson, R. Naylor, and S. Polasky. 2002. "Agricultural Sustainability and Intensive Production Practices." *Nature* 418: 671–677.
- USDA. 2010. United States Department of Agriculture. Foreign Agricultural Service. Accessed May 21, 2015. www.fas.usda.gov/psdonline/.
- Velpuri, N. M., P. S. Thenkabail, M. K. Gumma, C. B. Biradar, P. Noojipady, V. Dheeravath, and L. Yuanjie. 2009. "Influence of Resolution in Irrigated Area Mapping and Area Estimations." *Photogrammetric Engineering & Remote Sensing* 75: 1383–1395.
- World Bank. 2015. PovcalNet. Accessed May 25, 2015. <http://iresearch.worldbank.org/PovcalNet/povcalNet.html>.
- Xu, C.-Y., L. Gong, T. Jiang, D. Chen, and V. Singh. 2006. "Analysis of Spatial Distribution and Temporal Trend of Reference Evapotranspiration and Pan Evaporation in Changjiang (Yangtze River) Catchment." *Journal of Hydrology* 327: 81–93.
- Zheng, B., S. W. Myint, P. S. Thenkabail, and R. M. Aggarwal. 2015. "A Support Vector Machine to Identify Irrigated Crop Types Using Time-series Landsat NDVI Data." *International Journal of Applied Earth Observation and Geoinformation* 34: 103–112.